MNRAS 000, 1–7 (2022) Preprint 24 January 2022 Compiled using MNRAS LATEX style file v3.0

Pulsating hydrogen-deficient white dwarfs and pre-white dwarfs observed with TESS – IV. Discovery of two new GW Vir stars: TIC 0403800675 and TIC 1989122424

Murat Uzundag,[1,2]★, Alejandro H. Córsico[3,4], S. O. Kepler[5], Leandro G. Althaus[3,4], Klaus Werner[6], Nicole Reindl[7] and Maja Vučković[1]

[1]*Instituto de Física y Astronomía, Universidad de Valparaíso, Gran Bretaña 1111, Playa Ancha, Valparaíso 2360102, Chile*
[2]*European Southern Observatory, Alonso de Cordova 3107, Santiago, Chile*
[3]*Grupo de Evolución Estelar y Pulsaciones. Facultad de Ciencias Astronómicas y Geofísicas, Universidad Nacional de La Plata, Paseo del Bosque s/n, 1900, Argentina*
[4]*IALP - CONICET*
[5]*Instituto de Física, Universidade Federal do Rio Grande do Sul, 91501-970, Porto-Alegre, RS, Brazil*
[6]*Institut für Astronomie und Astrophysik, Kepler Center for Astro and Particle Physics, Eberhard Karls Universität, Sand 1,72076 Tübingen, Germany*
[7]*Institute for Physics and Astronomy, University of Potsdam, Karl-Liebknecht-Str. 24/25, D-14476 Potsdam, Germany*

Accepted XXX. Received YYY; in original form ZZZ

ABSTRACT

We present two new GW Vir-type pulsating white dwarf stars, TIC 0403800675 (WD J115727.68-280349.64) and TIC 1989122424 (WD J211738.38-552801.18) discovered in the Transiting Exoplanet Survey Satellite (TESS) photometric data. For both stars the TESS light curves reveal the presence of oscillations with periods in a narrow range between 400 and 410 s, which are associated with typical gravity (g)-modes. Follow-up ground-based spectroscopy shows that both stars have similar effective temperature ($T_{\rm eff} = 110,000 \pm 10,000$ K) and surface gravity ($\log g = 7.5 \pm 0.5$), but different He/C composition: He = 0.75 and C = 0.25 for TIC 0403800675, and He = 0.50 and C = 0.50 for TIC 1989122424. By performing a fit to their spectral energy distributions, we found for both stars radii and luminosities of $R = 0.019 \pm 0.002\,R_\odot$ and $\log(L/L_\odot) = 1.68^{+0.15}_{-0.24}$, respectively. Employing state-of-the-art evolutionary tracks of PG 1159 stars, we find a stellar mass of for both stars of $0.56^{+0.15}_{-0.05} M_\odot$ from the Kiel-diagram and $0.60^{+0.11}_{-0.09} M_\odot$ from the Hertzsprung Russell diagram.

Key words: stars — pulsations — stars: interiors — stars: evolution — stars: white dwarfs

1 INTRODUCTION

White dwarf (WD) stars are the end evolutionary state of all stars formed with initial masses below around $7-11\,M_\odot$, which comprise more than 95% of all stars in our galaxy (Althaus et al. 2010). In the course of their evolution, WDs cross at least one phase of pulsational instability that converts them into pulsating variable stars. GW Vir variable stars are the hottest known class of pulsating WDs and pre-WDs, with $75\,000\ {\rm K} \leq T_{\rm eff} \leq 250\,000$ K and $5.3 \leq \log g \leq 8$ (Werner et al. 2021). They are located within a definite instability strip (see Fig. 1 of Córsico et al. 2019). GW Vir stars include some objects that are still surrounded by a nebula, called the variable planetary nebula nuclei (PNNVs), and some objects that lack a nebula, which are called DOVs. Both groups (DOVs and PNNVs) are frequently referred to as GW Vir variable stars. GW Vir stars display brightness fluctuations with periods in the range 300 – 6 000 s, and amplitudes up to a few mmag (1 mmag=1 ppt), associated to low-order ($\ell \leq 2$) non-radial g(gravity) modes.

GW Vir stars are pulsating PG 1159 stars (after the prototype of the spectroscopic class, the star PG 1159−035), which are hydrogen(H)-deficient post-AGB stars with surface layers rich in helium (He), carbon (C) and oxygen (O) (Werner & Herwig 2006). It is believed that this mixture is a result of a mixing event produced by a late He flash during the so-called born-again episode (Althaus et al. 2010). PG 1159 stars are considered the evolutionary link between post-AGB stars and most of the H-deficient WDs, including DO and DB WDs (Althaus et al. 2005; Bédard et al. 2020; Sowicka et al. 2021). They can be either the outcome of single star evolution (late thermal pulse scenario, LTP, or very late thermal pulse scenario, VLTP) or binary star evolution (double WD merger). The classification of GW Vir stars includes also the pulsating Wolf-Rayet central stars of a planetary nebula ([WC]) and Early-[WC] = [WCE] stars since they share the same pulsation properties of pulsating PG 1159 stars (Quirion et al. 2007). PG 1159 stars are rare, and around 50 of them have been found so far (Werner et al. 2021). Amongst them, approximately 50% (22 objects; see Córsico et al. 2019; Uzundag et al. 2021) have been discovered to be pulsating. It is especially important to find new pulsators of this class, as they can provide insight into the AGB and VLTP/LTP phases, as well as angular momentum loss throughout the extensive mass loss phases (Kepler et al. 2014, and references therein).

Prior to space missions, GW Vir stars were monitored through

★ E-mail: murat.uzundag@postgrado.uv.cl

long-term observations carried out by the multisite photometric campaign with the "Whole Earth Telescope" (WET; Nather et al. 1990). These observations provided invaluable sources of information to constrain their internal structure (Winget et al. 1991). The spectral observations from the Sloan Digital Sky Survey (SDSS, York et al. 2000) promoted the discovery of a GW Vir pulsating star, SDSS J075415.12+085232.18 (Kepler et al. 2014). The advent of the *Kepler* space mission has resulted in important advances in the study of pulsating stars in general (Aerts 2021), and pulsating WDs in particular (Córsico 2020). Unfortunately, during the main mission of the *Kepler* satellite (Borucki et al. 2010), no GW Vir star was observed. During the *Kepler* extended mission (*K2*; Howell et al. 2014), the prototypical star PG 1159−035 was observed during almost 50 days of coverage, showing around 200 frequencies and strong nonlinear effects throughout the observations. Unfortunately, these results have not yet been published. Currently, uninterrupted observations from space with the Transiting Exoplanet Survey Satellite (TESS) allow us to find and characterize new and already known GW Vir stars. Indeed, TESS has allowed a detailed asteroseismological analysis of a number of formerly known GW Vir stars (Córsico et al. 2021b), enabling the determination of their fundamental parameters and evolutionary properties. The discovery of two new GW Vir stars has been presented by Uzundag et al. (2021). In these studies, using asteroseismic techniques (e.g., asymptotic period spacing and rotational splittings), the authors were able to determine the internal chemical stratification, total mass and, in some cases, rotation velocity of GW Vir stars.

In this work, we present the discovery of two new GW Vir stars, TIC 0403800675 (WD J115727.68-280349.6) and TIC 198912242 (WD J211738.38-552801.1), which were observed during the survey phase of the southern ecliptic hemisphere cycle 1 and 3 of TESS. In addition, for each target we obtained low-resolution spectra and fitted model atmospheres to estimate their fundamental atmospheric parameters, and examined the TESS light curve to identify the pulsational modes. This study is the fourth part of a series of papers devoted to the study of pulsating H-deficient WDs and pre-WDs observed with TESS. The first article was devoted to a set of six already known GW Vir stars (Córsico et al. 2021b), the second one to the discovery of two new GW Vir stars (Uzundag et al. 2021), and the third one to an detailed asteroseismological analysis of the prototype of the pulsating DB WD, GD 358 (Córsico et al. 2021a).

The paper is organized as follows. In Sect. 2, we present the details of spectroscopic observations and the data reduction. In Sect. 3, we derive atmospheric parameters for each star by fitting synthetic spectra to the newly obtained low-resolution spectra. In Sect. 5, we analyze the photometric TESS data and give details on the frequency analysis. Finally, in Sect. 6, we summarize our main results.

2 SPECTROSCOPY

TIC 0403800675 (WD J115727.68280349.6) and TIC 198912242 (WD J211738.38552801.1) were classified as WD candidates by Gentile Fusillo et al. (2019) from their colors and Gaia DR2 parallax. The Gaia DR3 parallax and corresponding distance for TIC 0403800675 are $\pi = 1.86^{+0.07}_{-0.06}$ mas and $d = 535.41^{+19.49}_{-18.44}$ pc, while for TIC 198912242 are $\pi = 1.45^{+0.05}_{-0.06}$ mas and $d = 688.27^{+22.34}_{-26.31}$ pc (Bailer-Jones et al. 2021), respectively.

To estimate the atmospheric parameters of TIC 0403800675 and TIC 1989122424, we obtained spectra with the Goodman High-Throughput Spectrograph (GHTS, Clemens et al. 2004) at the SOAR 4.1-m telescope on Cerro Pachón. We reduced the spectroscopic data using the instrument pipeline[1] including overscan, trim, slit trim, bias and flat corrections. We employed a method developed by Pych (2004), which is included in the pipeline, to identify and remove cosmic rays. After the reduction was completed, the wavelength has been applied by using *PyRAF*[2] (Science Software Branch at STScI 2012). We used the frames produced with the internal He-Ar-Ne comparison lamp at the same telescope position as the targets in order to apply wavelength calibrations. The sixth order Legendre function is used to calibrate the pixel-wavelength correspondence using an atlas of known He-Ar-Ne lines. Finally, we used the standard star of Feige 110 seen with the identical apparatus to normalize the spectra with a high-order Legendre function. Table 1 contains the details of the spectroscopic observations, including the name of the targets, right ascension, declination, Gaia magnitude, date, exposure time, grating, resolution, and S/N ratio.

3 SPECTRAL FITTING

The spectral lines in the spectra of TIC 0403800675 and TIC 1989122424 are all from He II and C IV. Oxygen, which is the most abundant element in PG 1159 stars after He and C, and nitrogen (N) —which is present as a trace element in some PG 1159 stars— may be visible in spectra with higher resolution and signal-to-noise ratio. In the spectra of both stars, there are no indications of the presence of H.

For the spectral analysis, we used a grid of line-blanketed non-local thermodynamic equilibrium (non-LTE) model atmospheres consisting of H, He, and C as introduced by Werner et al. (2014). The grid spans $T_{\rm eff}$ = 60,000–140,000 K in effective temperature and $\log g$ = 4.8–8.3 in surface gravity, with steps of 5,000 K or 10,000 K and 0.3 dex, respectively. C/He mass ratios in the range 0.0–1.0 were considered, namely C/He = 0.0, 0.03, 0.09, 0.33, 0.77, and 1.0. Synthetic spectra were convolved with a Gaussian accounting for the spectral resolution of the observations. The best fitting models were chosen by visual comparison with the rectified observed spectra.

The model fits are depicted in Fig. 1. Both stars have $T_{\rm eff} = 110,000 \pm 10,000$ K and $\log g = 7.5 \pm 0.5$, but a different atmospheric composition. For TIC 0403800675, we found He = $0.75^{+0.05}_{-0.15}$ and C = $0.25^{+0.15}_{-0.05}$ and for TIC 1989122424, we measured He = $0.50^{+0.20}_{-0.05}$ and C = $0.50^{+0.05}_{-0.20}$ (mass fractions). In Fig. 3 we show the location of the new GW Vir stars in the Kiel diagram. By linear interpolation among the PG 1159 evolutionary tracks of Miller Bertolami & Althaus (2006), we derive a stellar mass of $M_\star = 0.56^{+0.15}_{-0.05} M_\odot$ for TIC 0403800675 and TIC 1989122424.

4 SED FITTING

In order to determine the radii of the two stars we performed a fit to the spectral energy distribution (SED), by varying the solid angle $\pi(R/d)^2$, (which relates the flux at the surface of the system to what is received at Earth) until a good agreement of the synthetic fluxes and the observations was found (Fig.4). We employed our best fitting model atmospheres for both stars, and using the Fitzpatrick (1999) reddening law, our synthetic spectra were reddened for different values of $E_{\rm B-V}$. We used the distance provided by Bailer-Jones et al. (2021) and employed photometry from Galex (Bianchi et al. 2014),

[1] https://github.com/soar-telescope/goodman_pipeline
[2] http://www.stsci.edu/institute/software_hardware/pyraf

Table 1. Log of spectroscopic observations.

TIC	Name	RA (J2000)	Dec (J2000)	G_{mag}	Obs. Date (UT)	Exp. (sec)	Grating (l mm^{-1})	Resolution ($\Delta\lambda$ (Å))	S/N
0403800675	WD J115727.68−280349.64	11:57:28	-28:03:53	16.16	2021-06-18 03:26:17	1200	400	4.6	65
1989122424	WD J211738.38−552801.18	21:17:40	-55:28:16	16.75	2021-06-19 07:54:54	900	400	4.6	70

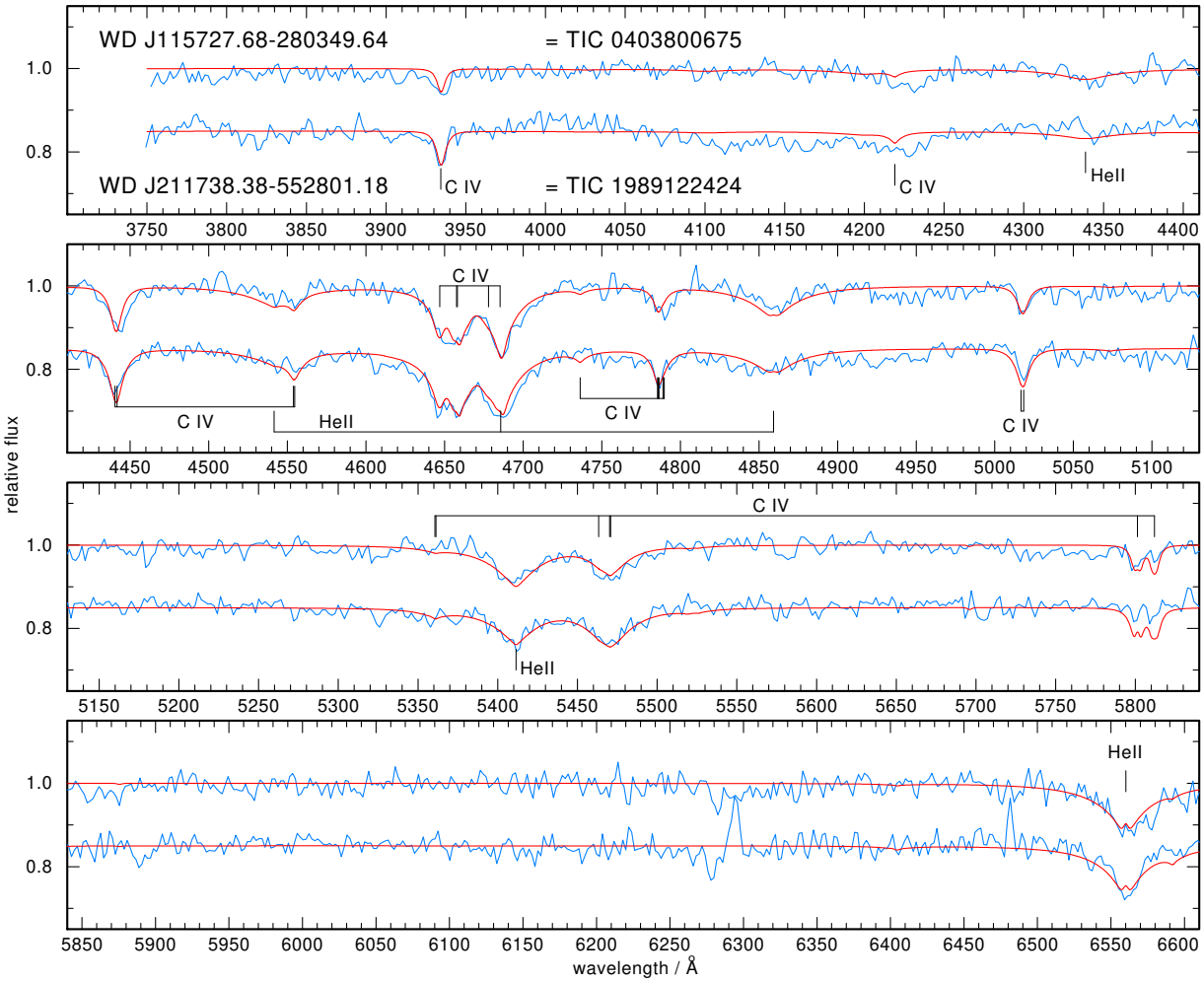

Figure 1. Optical spectra of the two new GW Vir stars (blue graphs) obtained with SOAR/Goodman. Overplotted are the best-fit models (red). Identifications of He II and C IV lines are marked.

Gaia DR2 and eDR3 (Gaia Collaboration et al. 2021), and Pan-STARRS1 (Chambers et al. 2016). Magnitudes were converted into fluxes using the VizieR Photometry viewer[3]. For TIC 0403800675 we find a reddening of $E_{B-V} = 0.034$ mag and for TIC 1989122424 we find $E_{B-V} = 0.048$ mag. Both values are in agreement with the upper limits of the 2D dust map provided by Schlafly & Finkbeiner (2011). For both stars we determine a radius of $R = 0.019 \pm 0.002\, R_\odot$. Using $L = 4\pi\,\sigma R^2 T_{\rm eff}^4$, where σ is the Stefan-Boltzmann constant, we calculate for both stars a luminosity of $\log(L/L_\odot) = 1.68^{+0.15}_{-0.24}$. This allows us now to also derive the masses for TIC 0403800675 and TIC 1989122424 in the HRD. By linear interpolation among the PG 1159 evolutionary tracks of Miller Bertolami & Althaus (2006), we derive a stellar mass of $M_\star = 0.60^{+0.11}_{-0.09} M_\odot$ for both stars, and which is in agreement with the masses derived from the Kiel diagram (see Fig.3). The main characteristics of TIC 0403800675 and TIC 1989122424 are listed in Table 2 including atmospheric parameters, masses, luminosities, radii, distances and reddening.

[3] http://vizier.unistra.fr/vizier/sed/

5 PHOTOMETRIC OBSERVATIONS — TESS

TIC 0403800675 was observed in sector 10 between 26 March to 22 April 2019 and in sector 36 between 7 March and 2 April 2021.

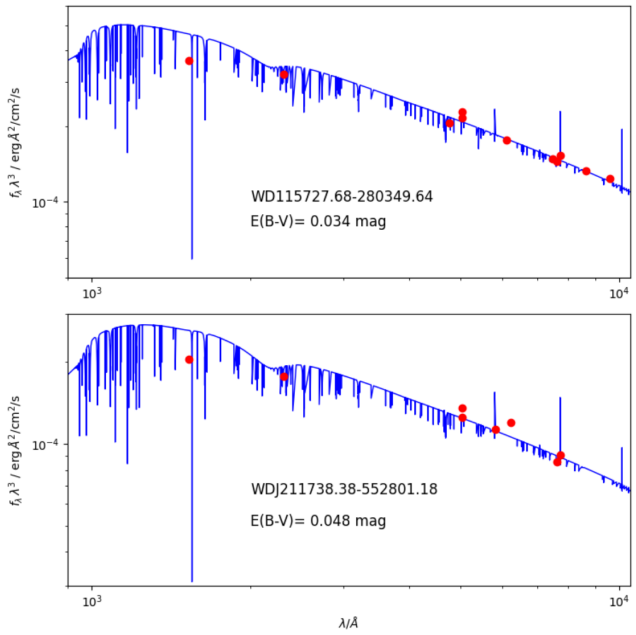

Figure 2. Comparison of our best fitting model fluxes (blue) with the observed photometry (red).

Table 2. Properties of GW Vir pulsating stars studied in this work.

Quantity	TIC 0403800675	TIC 1989122424
$T_{\rm eff}$ [kK]	110 ± 10	110 ± 10
$M_\star$ [$M_\odot$]	$0.56^{+0.15}_{-0.05}$	$0.56^{+0.15}_{-0.05}$
$\log g$ [cm/s^2]	7.5 ± 0.5	7.5 ± 0.5
(He, C)	$0.75^{+0.05}_{-0.15}$, $0.25^{+0.15}_{-0.05}$	$0.50^{+0.20}_{-0.05}$, $0.50^{+0.05}_{-0.20}$
$R_\star$ [$R_\odot$]	0.019 ± 0.002	0.019 ± 0.002
$\log(L_\star/L_\odot)$	$1.68^{+0.15}_{-0.24}$	$1.68^{+0.15}_{-0.24}$
$E(B-V)$ [mag]	0.034	0.048
π [mas]	$1.86^{+0.07}_{-0.06}$	$1.45^{+0.05}_{-0.06}$
d [pc]	$535.41^{+19.49}_{-18.44}$	$688.27^{+22.34}_{-26.31}$

TIC 1989122424 was observed in a single sector 27 between 4 July and 30 July 2020 with only 120 sec cadence.

The light curves were downloaded from The Mikulski Archive for Space Telescopes, which is hosted by the Space Telescope Science Institute (STScI)[4] as FITS format. The light curves were processed by the Science Processing Operations Center (SPOC) pipeline (Jenkins et al. 2016). We first downloaded the target pixel file (TPF) of interest from the MAST archive, which is maintained by the Lightkurve Collaboration; Lightkurve Collaboration et al. (2018). The TPFs comprises an 11x11 postage stamp of pixels from the one of four CCDs per camera that the target is located on. The TPFs are examined to determine the amount of crowding and other potential bright sources near the target. Because both targets had a modest amount of crowding which we evaluated using the `CROWDSAP` parameter, that was set to 0.6 for TIC 1989122424 and 0.8 for TIC 0403800675. Therefore we have decided to use the pipeline aperture as it gave the most optimal result with respect to signal-to-noise ratio. We extracted times in barycentric corrected dynamical Julian days and fluxes (PDCSAP FLUX) from the FITS files. We converted the fluxes to fractional variations from the mean and transformed to amplitudes in parts-per-thousand (ppt). Finally, the data were sigma-clipped based on 5 σ to remove the outliers which appear above 5 times the median of intensities. The resulting short-cadence (SC) light curve of TIC 040380067 comprises 29 298 images spanning 47.4 days, while the resulting SC light curve of TIC 1989122424 includes 16 478 data points spanning 23.9 days. TIC 0403800675 was also observed with ultra-short-cadence (USC) during 23.9 days in sector 36 that yield 93 122 images.

[4] http://archive.stsci.edu/

5.1 Frequency solution

The Fourier transform (FT) was utilized in order to examine the periodicities present in the light curves. We used both the `Period04` and our custom tool to calculate each FT and fit each pulsational frequency that appears above the 0.1% false alarm probability (FAP). The FAP level was calculated by reshuffling the light curves 1000 times as described in (Kepler 1993). The errors of each frequency and amplitude of the pulsation modes were estimated using Monte Carlo simulations (Lenz & Breger 2005). Furthermore, we have calculated sliding Fourier transform (sFT) for both stars in order to see the temporal evolution of the pulsational modes over the course of TESS observations. To do so, we use a nine-day sliding window with a 2-day step size. A color-scale in ppt units is used to depict the amplitudes. Following that, we calculate the Fourier transform of each subset and trail them in time.

For TIC 0403800675, we analyzed TESS observations using the SC and USC modes. The SC mode samples every 2-minutes allowing us to analyze the frequency range up to the Nyquist frequency at about 4167 μHz, while the USC mode samples every 20-seconds permitting us to examine the frequency range up to the Nyquist frequency at about 25 000 μHz. For TIC 0403800675, we detected two significant frequencies at 2445 μHz and 2450 μHz. In Fig.4, we show FT of combined SC data of sector 10 and 36 (black lines) (top panel), while the middle panel, we present USC data of sector 36. The magenta lines show the FT of the prewhitened light curves. The signals are 20% more amplified in USC data. Sliding Fourier transform display the both identified peaks in Fig.4. The frequencies detected for TIC 0403800675 are presented in Table 3.

For TIC 1989122424, we also detected two clear signals at similar region between 2450 μHz and 2490 μHz using solely SC observations. In Fig.5, we focus on this region and show the FT of the original light curve (black line) and the FT of the prewhitened light curves (magenta line). In sFT, these peaks also clearly visible along with some other peaks. The two reported peaks at 2466 μHz and 2479 μHz are clearly visible in sFT and they are stable during the run. We also see that there is a peak at 2470 μHz, which is stable during the first ten days. For this peak, we did not produce an NLLS fit to extract from the light curve. We need additional observations to confirm whether it is real pulsational peak or not. The detected frequencies for TIC 0403800675 are reported in Table 4.

Unfortunately, the presence of only two oscillation frequencies in the power spectrum of each star prevents us from carrying out an asteroseismological modeling on these objects. We hope that more periods can be detected in the future, so that we can investigate the internal structure and evolutionary state of these stars through asteroseismological tools.

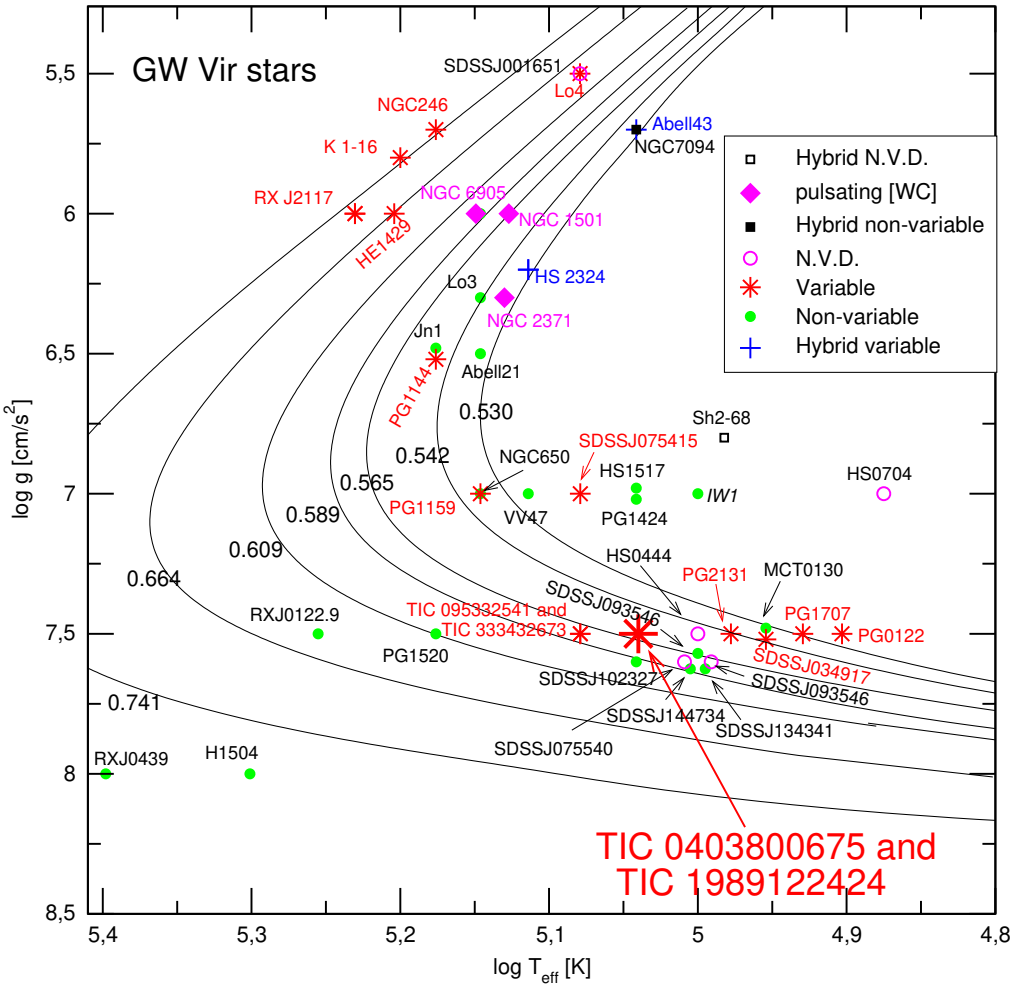

Figure 3. The already known variable and non-variable PG 1159 stars and variable [WCE] stars in the $\log T_{\rm eff} - \log g$ diagram. Thin solid curves show the post-born again evolutionary tracks from Miller Bertolami & Althaus (2006) for different stellar masses. "N.V.D." stands for PG 1159 stars with no variability data. "Hybrid" refers to PG 1159 stars exhibiting H in their atmospheres. The location of the two new GW Vir stars TIC 0403800675 and TIC 1989122424 is emphasized with a large red star symbol. Both stars share the same spectroscopic surface parameters, $T_{\rm eff} = 110\,000 \pm 10\,000$ K and $\log g = 7.5 \pm 0.5$.

Table 3. Identified frequencies, periods, and amplitudes (and their uncertainties) and the signal-to-noise ratio in the data of TIC 0403800675. Frequency and amplitude that are detected in both sector 10 and 36.

Peak	ν (μHz)	Π (s)	A (ppt)	S/N
f_1	2443.597(51)	409.232(86)	1.63(33)	4.3
f_2	2449.261(33)	408.286(55)	2.54(33)	6.3

Table 4. Identified frequencies, periods, and amplitudes (and their uncertainties) and the signal-to-noise ratio in the data of TIC 1989122424.

Peak	ν (μHz)	Π (s)	A (ppt)	S/N
f_1	2466.673(41)	405.404(68)	18.35(2.89)	5.1
f_2	2479.888(44)	403.243(72)	16.99(2.89)	4.7

6 CONCLUSIONS

In this paper, we have presented the discovery of two new GW Vir pulsating white dwarfs TIC 0403800675 and TIC 1989122424. We derived atmospheric parameters for TIC 0403800675 and TIC 1989122424 by fitting synthetic spectra to the newly obtained low-resolution SOAR/GOODMAN spectra. The determined spectroscopic parameters demonstrate that TIC 0403800675 and TIC 1989122424 are identical in terms of surface temperature and surface gravity ($T_{\rm eff} = 110,000 \pm 10,000$ K and $\log g = 7.5 \pm 0.5$) and they are only different regarding the surface C and He abundance. By performing a fit to the SEDs we found for both stars radii and luminosities of $R = 0.019 \pm 0.002\,R_\odot$ and $\log(L/L_\odot) = 1.68^{+0.15}_{-0.24}$, respectively. Using state-of-the-art evolutionary tracks of PG 1159 stars, we find a stellar mass of for both stars of $0.56^{+0.15}_{-0.05} M_\odot$ from the Kiel-diagram and $0.60^{+0.11}_{-0.09} M_\odot$ from the HRD.

We have utilized the TESS 120-second data for both objects, while we made use of 20-second cadence data for only TIC 0403800675. Both stars exhibit just two periodicities in their amplitude spectra preventing us to make use of the seismic tools of rotational multiplets and asymptotic period spacing. Both pulsational frequencies that we extracted from the light curves are of the order of 7 minutes,

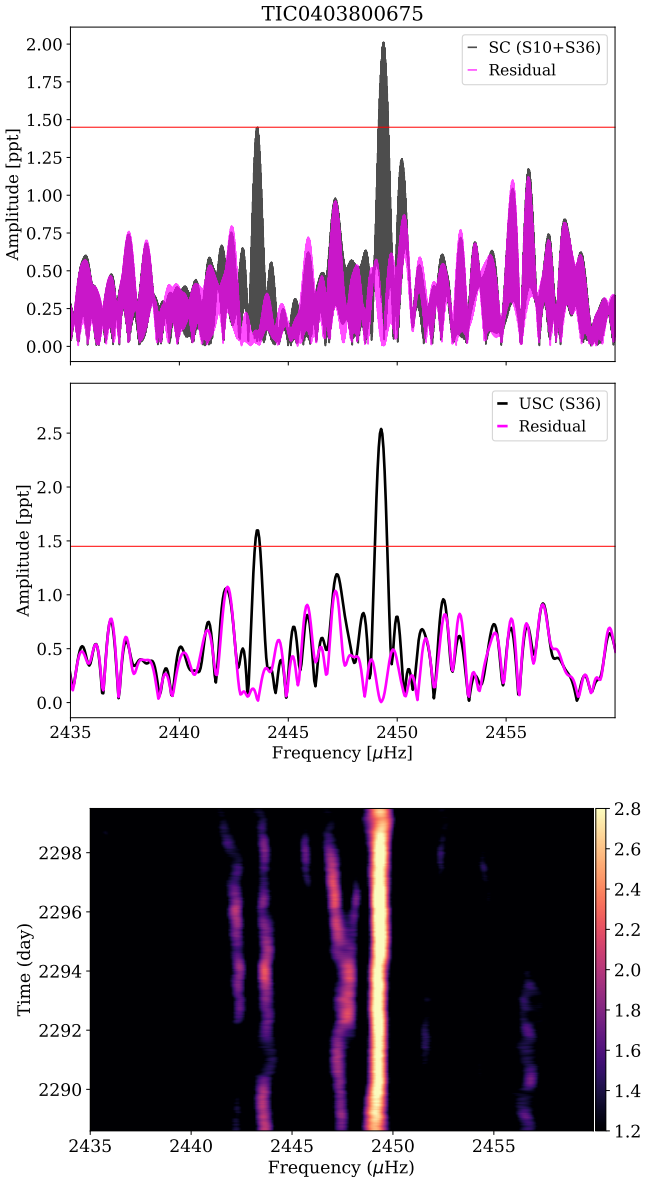

Figure 4. Top: Fourier transform of short-cadence data of sector 10 and 36 (black lines). The magenta line depicts the FT of the prewhitened light curve. The horizontal red line indicates the 0.1% FAP level. Middle: Fourier transform of ultra-short-cadence data of sector 36 (black lines) for TIC 0403800675. The red and magenta lines are the same as top panel the 0.1% FAP level and the FT of the prewhitened light curve, respectively. Bottom: Sliding Fourier transform of ultra-short-cadence data of sector 36 data of TIC 0403800675. The color-scale illustrates amplitude in ppt units.

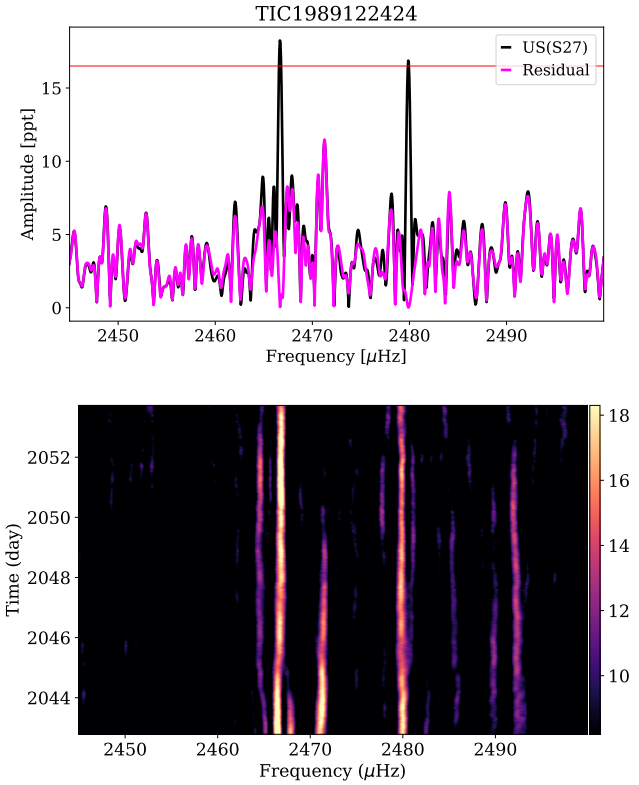

Figure 5. Top: Fourier transform of short-cadence data of sector 27 of TIC 1989122424. The horizontal red line indicates the 0.1% FAP level. The magenta line depicts the FT of the prewhitened light curve. Bottom: Sliding Fourier transform of the same data-set of TIC 1989122424. The color-scale illustrates amplitude in ppt units.

attributable to non-radial pulsation g-modes. We also produced sFTs to see if the pulsation modes are resolved and stable throughout the TESS observations, which is limited to a single sector. The analyzed data demonstrate that the main pulsational frequencies of our targets are stable and there is no clear pattern for rotational multiplets. However, the two closely separated peaks might be a result of rotational multiplets of dipole or quadrupole modes. Assuming these frequencies are dipole modes and result from a stellar rotation, then the rotation rates would be ranging from 1.02 to 2.04 d (depending on the missing azimuthal order) for TIC 0403800675 and 0.43 d to 0.87 d for TIC 1989122424. Given the rotation rates of the GW Vir pulsating stars, which range from 5 hours to a few days (Córsico et al. 2019, 2021b), any of the potential solutions that we estimate for TIC 0403800675 and TIC 1989122424 could be conceivable.

We also note that the rotational periods of GW Vir stars cover about the same period range as white dwarfs showing ultra-highly excited (UHE) metals in their optical spectra. Reindl et al. (2021) discovered recently that this latter class of white dwarfs show photometric periods between 6 hours to 3 days and that their variability is likely caused by spots on the surfaces of these stars and/or geometrical effects of circumstellar material (see also Reindl et al. 2019). Since UHE white dwarfs are considered to be in an evolutionary stage immediately following that of the GW Vir pulsators, it would be interesting to know the rotational periods of more GW Vir stars in order to test a possible evolutionary connection.

GW Vir stars evolve quickly, resulting in a significant period change due to cooling and contraction, which should be detected in a few years. As a result, these stars can be checked at least once a year to determine evolutionary changes as described by Costa & Kepler (2008).

ACKNOWLEDGEMENTS

M.U. acknowledges financial support from CONICYT Doctorado Nacional in the form of grant number No: 21190886 and ESO stu-

dentship program. M.U. thanks Aleksandar Cikota for valuable discussions. Based on observations obtained at the Southern Astrophysical Research (SOAR) telescope under the program allocated by the Chilean Time Allocation Committee (CNTAC), no:CN2020A-87, CN2020B-74 and CN2021A-52. This paper includes data collected with the TESS mission, obtained from the MAST data archive at the Space Telescope Science Institute (STScI). Funding for the TESS mission is provided by the NASA Explorer Program. This work has made use of data from the European Space Agency (ESA) mission Gaia (https://www.cosmos.esa.int/gaia), processed by the Gaia Data Processing and Analysis Consortium (DPAC, https://www.cosmos.esa.int/web/gaia/dpac/consortium). Funding for the DPAC has been provided by national institutions, in particular the institutions participating in the Gaia Multilateral Agreement. Part of this work was supported by AGENCIA through the Programa de Modernización Tecnológica BID 1728/OC-AR,and by the PIP 112-200801-00940 grant from CONICET. This research has made use of NASA's Astrophysics Data System Bibliographic Services, and the SIMBAD database, operated at CDS, Strasbourg, France.

DATA AVAILABILITY

Data from TESS is available at the MAST archive https://mast.stsci.edu/search/hst/ui/$#$/. Ground based data will be shared on reasonable request to the corresponding author.

REFERENCES

Aerts C., 2021, Reviews of Modern Physics, 93, 015001
Althaus L. G., Serenelli A. M., Panei J. A., Córsico A. H., García-Berro E., Scóccola C. G., 2005, A&A, 435, 631
Althaus L. G., Córsico A. H., Isern J., García-Berro E., 2010, A&ARv, 18, 471
Bailer-Jones C. A. L., Rybizki J., Fouesneau M., Demleitner M., Andrae R., 2021, VizieR Online Data Catalog, p. I/352
Bédard A., Bergeron P., Brassard P., Fontaine G., 2020, ApJ, 901, 93
Bianchi L., Conti A., Shiao B., 2014, VizieR Online Data Catalog, 2335, 0
Borucki W. J., et al., 2010, Science, 327, 977
Chambers K. C., et al., 2016, arXiv e-prints, p. arXiv:1612.05560
Clemens J. C., Crain J. A., Anderson R., 2004, in Moorwood A. F. M., Iye M., eds, Society of Photo-Optical Instrumentation Engineers (SPIE) Conference Series Vol. 5492, Ground-based Instrumentation for Astronomy. pp 331–340, doi:10.1117/12.550069
Córsico A. H., 2020, Frontiers in Astronomy and Space Sciences, 7, 47
Córsico A. H., Althaus L. G., Miller Bertolami M. M., Kepler S. O., 2019, A&ARv, 27, 7
Córsico A. H., et al., 2021a, arXiv e-prints, p. arXiv:2111.15551
Córsico A. H., et al., 2021b, A&A, 645, A117
Costa J. E. S., Kepler S. O., 2008, A&A, 489, 1225
Fitzpatrick E. L., 1999, PASP, 111, 63
Gaia Collaboration et al., 2021, A&A, 650, C3
Gentile Fusillo N. P., et al., 2019, MNRAS, 482, 4570
Howell S. B., et al., 2014, PASP, 126, 398
Jenkins J. M., et al., 2016, in Software and Cyberinfrastructure for Astronomy IV. p. 99133E, doi:10.1117/12.2233418
Kepler S. O., 1993, Baltic Astronomy, 2, 515
Kepler S. O., Fraga L., Winget D. E., Bell K., Córsico A. H., Werner K., 2014, Monthly Notices of the Royal Astronomical Society, 442, 2278
Lenz P., Breger M., 2005, Communications in Asteroseismology, 146, 53
Lightkurve Collaboration et al., 2018, Lightkurve: Kepler and TESS time series analysis in Python (ascl:1812.013)
Miller Bertolami M. M., Althaus L. G., 2006, A&A, 454, 845
Nather R. E., Winget D. E., Clemens J. C., Hansen C. J., Hine B. P., 1990, ApJ, 361, 309
Pych W., 2004, PASP, 116, 148
Quirion P. O., Fontaine G., Brassard P., 2007, ApJS, 171, 219
Reindl N., et al., 2019, MNRAS, 482, L93
Reindl N., Schaffenroth V., Filiz S., Geier S., Pelisoli I., Kepler S. O., 2021, A&A, 647, A184
Schlafly E. F., Finkbeiner D. P., 2011, ApJ, 737, 103
Science Software Branch at STScI 2012, PyRAF: Python alternative for IRAF (ascl:1207.011)
Sowicka P., Handler G., Jones D., van Wyk F., 2021, ApJ, 918, L1
Uzundag M., et al., 2021, A&A, 655, A27
Werner K., Herwig F., 2006, PASP, 118, 183
Werner K., Rauch T., Kepler S. O., 2014, A&A, 564, A53
Werner K., Reindl N., Dorsch M., Geier S., Munari U., Raddi R., 2021, arXiv e-prints, p. arXiv:2111.13549
Winget D. E., et al., 1991, ApJ, 378, 326
York D. G., et al., 2000, AJ, 120, 1579

This paper has been typeset from a TEX/LATEX file prepared by the author.